AIMS Biophysics, 9(1): 61–71.
DOI: 10.3934/biophy.2022006
Received: 20 January 2022
Revised: 27 February 2022
Accepted: 07 March 2022
Published: 18 March 2022

http://www.aimspress.com/journal/biophysics

Research article

Density of electric field energy around two surface-charged spheres surrounded by electrolyte II. The smaller sphere is inside the larger one

István P. Sugár*

Department of Neurology, Icahn School of Medicine at Mount Sinai, New York, NY 10029

* **Correspondence:** Email: istvansugar0@gmail.com.

Abstract: Based on the generalized version of Newton's Shell Theorem [7] the electric field energy density, u_F around two surface-charged spheres surrounded by electrolyte where the smaller sphere is inside the larger one is analytically calculated. According to the calculations when the surfaces of the spheres are farther from each other than four times of the Debye length the field energy density around and inside the smaller sphere is basically independent from the presence of the larger sphere. The electric field energy density is maximal when the smaller sphere touches the inner surface of the larger sphere and the maximum of u_F is located at the touching point on the outer surface of the larger sphere.

Keywords: generalized shell theorem; electric field energy density; Debye length

1. Introduction

The head groups of membrane lipids have either single charge (e.g. tetraether lipids [1], phosphatidic acid (PA), phosphatidylserine (PS), phosphatidylethanolamine (PE), and phosphatidylinositol (PI)) or electric dipole (e.g. phospholipids, such as dimyristoyl-, dipalmitoyl- and distearoylphosphatidyl choline (DMPC, DPPC and DSPC, respectively)).

Between lipids containing head groups with electric dipole there is short range interaction, i.e. where the two-body potential decays algebraically at large distances with a power equal or larger than the spatial dimension [2]. Theoretical models of lipid membranes usually focus on systems where there is short range lateral interactions between nearest neighbor lipids [3,4] because it is enough to consider only the interactions between nearest-neighbor lipid molecules. It is much more difficult to model a

lipid membrane containing single charged head groups [5]. Between lipids with single charged head groups there is long range interaction, i.e. where the two-body potential decays algebraically at large distances with a power smaller than the spatial dimension [2] and thus modeling this system one has to consider the entire system rather than the interactions between the nearest-neighbor lipids. In order to get closer to the solution of this problem recently we developed a generalized version of Newton's Shell Theorem [6,7] to calculate the electric potential, *V* around a surface-charged sphere (of radius R_1) surrounded by electrolyte at a distance *Z* from the center of the sphere (see also Eqs 9,10 in ref.7):

$$V(Z) = \frac{k_e \cdot Q_1 \cdot \lambda_D}{\varepsilon_r \cdot Z \cdot R_1} \cdot e^{-\frac{Z}{\lambda_D}} \cdot sinh\left(\frac{R_1}{\lambda_D}\right) \qquad at\ Z > R_1 \tag{1}$$

$$V(Z) = \frac{k_e \cdot Q_1 \cdot \lambda_D}{\varepsilon_r \cdot Z \cdot R_1} \cdot e^{-\frac{R_1}{\lambda_D}} \cdot sinh\left(\frac{Z}{\lambda_D}\right) \qquad at\ Z < R_1 \tag{2}$$

where $k_e = (4\,\pi\,\varepsilon_0)^{-1}$ is the Coulomb's constant, λ_D is the Debye length, Q_1 is the total charge of the homogeneously charged surface of the sphere of radius R_1, ε_r is the relative static permittivity of the electrolyte. Deriving Eqs.1,2 the general solution of the Screened Poisson Equation was utilized (see Eq 4 in ref.7 or A5 in Appendix 1), an equation that is valid if the electrolyte is electrically neutral [8]. It is important to note that the Screened Poisson Equation (Eq A4) is different from the Poisson-Boltzmann equation (see Eqs A1,A3). The Poisson-Boltzmann equation can be used to calculate the potential energy of an arbitrary, electroneutral, ion solution (i.e. electrolyte). However, for the solution (see Eq A2) one has to know the charge density of the ions in the electrolyte (i.e. the Boltzmann distribution; see Eq A3), which depends on the potential, *V*, itself. Thus only approximative solution is available (the Debye- Hückel approximation [9]), that is valid when $|z_i eV/(k_B T)| \ll 1$ (where e: charge of an electron, z_i: charge number of the i-th type of ion, k_B: Boltzmann constant, T: absolute temperature).

Using the Screened Poisson Equation (Eq A4) one can calculate the potential energy of an electrolyte that contains also external charges. The external charges are embedded into the electrolyte (like the charges of the surface-charged sphere) but not part of the electrolyte itself. For the solution one has to know the charge density of the external charges (see Eq 4 in ref.7 or Eq A5 in Appendix 1), i.e. distribution of the charges on the surface-charged sphere and not the distribution of the ions in the electrolyte. In our case it is assumed that the charges on the surface of the sphere are homogeneously distributed and in this case Eqs 1,2 is the exact solution of the Screened Poisson Equation.

Note that recently by using Eqs 1,2 electric energies have been calculated [10], such as the electric potential energy needed to build up a surface-charged sphere, and the field and polarization energy of the electrolyte inside and around the surface-charged sphere.

In this paper the density of electric field energy is calculated around two surface-charged spheres where the smaller sphere is located inside the larger one and the entire system is embedded in neutral electrolyte. This system is close to a charged vesicle [1] or to a cell [11] where charged lipids are located both on the outer and inner leaflet of the membrane, i.e. two concentric surface-charged spheres. It also models an eukaryote [12] where neutral phospholipids such as sphingomyelin and zwitterionic phosphatidylcholine are located primarily in the outer leaflet of the plasma membrane, and most anionic phospholipids, such as phosphatidic acid (PA), phosphatidylserine (PS), phosphatidylethanolamine (PE), and phosphatidylinositol (PI) are located in the inner leaflet of the plasma membrane (represented by the large surface-charged sphere of our model). Eukaryotes also have a single nucleus enveloped by double layer of lipid membranes which may contain charged lipids too (representing the smaller surface-charged sphere of our model). Note that these two charged

spheres of an eukaryote are not necessarily concentric. Finally, our model is generalized for the case when the large surface-charged sphere contains several smaller surface-charged spheres. This system may also model osteoclast cells [12] containing many nuclei.

In this work the density of the electric field energy inside and outside of two surface-charged spheres are calculated at different locations. The density of the electric field energy at a point can be calculated by the following equation [13]:

$$u_F = \frac{\varepsilon_r \varepsilon_0}{2} \underline{E} \cdot \underline{E} \tag{3}$$

where $\underline{E}$ is the vector of the electric field strength at the considered point, ε_0 is the absolute vacuum permittivity and ε_r is the relative permittivity of the electrolyte.

2. Model

Here by using the recently generalized Shell Theorem [7] we calculate the density of electric field energy, u_F produced by two surface-charged spheres (see Figure 1) surrounded outside and inside by electrolyte where the smaller sphere is located inside the larger sphere.

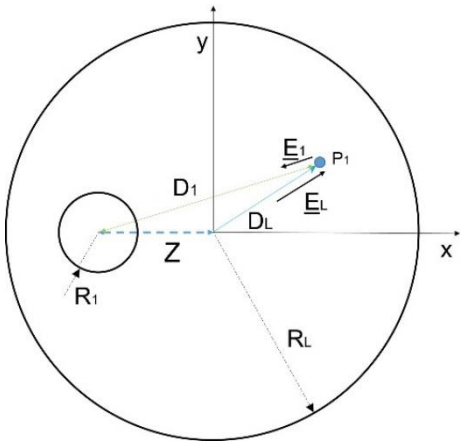

Figure 1. Two surface-charged spheres surrounded outside and inside by electrolyte where the smaller sphere is located inside the larger one.

Z: the distance between the centers of the spheres (dashed blue line); R_1 and R_L is the radius of the smaller and larger sphere, respectively; D_1 and D_L is the distance between point P_1 and the center of the smaller and larger sphere, respectively; $\underline{E}_1$ and $\underline{E}_L$ is the field strength created in point P_1 by the smaller and larger surface-charged sphere, respectively.

The origin of the coordinate system (x, y) is attached to the center of the larger sphere and the coordinates of point P_1 are x_p and y_p. The coordinates of the center of the larger and smaller sphere are $(x_L, y_L) = (0, 0)$ and $(x_1, y_1) = (-Z, 0)$, respectively.

In order to calculate the density of electric field energy one has to determine the electric field strength (see Eq 3), i.e. the gradient of the electric potential. The potential produced by the smaller sphere, V_1 at a distance D_1 from its center can be calculated by Eqs 1,2 (or Eqs 9,10 in ref.[7]). The electric field strength created by the smaller sphere at point P_1 (see Figure 1) is:

$$\underline{E_1} = -grad(V_1) = -(\frac{dV_1}{dD_1}\frac{dD_1}{dx_P}, \frac{dV_1}{dD_1}\frac{dD_1}{dy_P}) = -\frac{dV_1}{dD_1}(\frac{d\sqrt{(x_P-x_1)^2+(y_P-y_1)^2}}{dx_P}, \frac{d\sqrt{(x_P-x_1)^2+(y_P-y_1)^2}}{dy_P}) =$$

$$-\frac{dV_1}{dD_1}(\frac{x_P-x_1}{D_1}, \frac{y_P-y_1}{D_1}) = (-\frac{dV_1}{dD_1}\frac{x_P+Z}{D_1}, -\frac{dV_1}{dD_1}\frac{y_P}{D_1}) = (E_{1x}, E_{1y}) \quad (4)$$

where

$$\frac{dV_1}{dD_1} = \begin{cases} \frac{k_e Q_1 \lambda_D}{\varepsilon_r R_1} sinh(R_1/\lambda_D)\left[-\frac{e^{-\frac{D_1}{\lambda_D}}}{D_1^2} - \frac{e^{-\frac{D_1}{\lambda_D}}}{D_1 \lambda_D}\right] & if\ D_1 > R_1 \\ \frac{k_e Q_1 \lambda_D}{\varepsilon_r R_1} e^{-\frac{R_1}{\lambda_D}}\left[-\frac{sinh\left(\frac{D_1}{\lambda_D}\right)}{D_1^2} + \frac{cosh\left(\frac{D_1}{\lambda_D}\right)}{D_1 \lambda_D}\right] & if\ D_1 < R_1 \end{cases} \quad (5)$$

where λ_D is the Debye length and $Z \leq R_L - R_1$.

Similarly, the electric field strength created by the large sphere at point P1 (i.e. at a distance D_L from its center; see Figure 1) is:

$$\underline{E_L} = -grad(V_L) = -(\frac{dV_L}{dD_L}\frac{dD_L}{dx_P}, \frac{dV_L}{dD_L}\frac{dD_L}{dy_P})$$

$$= -\frac{dV_L}{dD_L}\left(\frac{d\sqrt{(x_P - x_L)^2 + (y_P - y_L)^2}}{dx_P}, \frac{d\sqrt{(x_P - x_L)^2 + (y_P - y_L)^2}}{dy_P}\right)$$

$$= -\frac{dV_L}{dD_L}\left(\frac{x_P - x_L}{D_L}, \frac{y_P - y_L}{D_L}\right) = \left(-\frac{dV_L}{dD_L}\frac{x_P}{D_L}, -\frac{dV_L}{dD_L}\frac{y_P}{D_L}\right) = \left(E_{Lx}, E_{Ly}\right) \quad (6)$$

where one can construct $\frac{dV_L}{dD_L}$ from Eq 5 by changing D_1 to D_L, R_1 to R_L and Q_1 to Q_L.

$$u_F(x_P, y_P) = \frac{\varepsilon_r \varepsilon_0}{2} \underline{E} \cdot \underline{E} = \frac{\varepsilon_r \varepsilon_0}{2} \left(\underline{E_1} + \underline{E_L}\right) \cdot \left(\underline{E_1} + \underline{E_L}\right)$$

$$= \frac{\varepsilon_r \varepsilon_0}{2} ([E_{1x} + E_{Lx}], [E_{1y} + E_{Ly}]) \cdot ([E_{1x} + E_{Lx}], [E_{1y} + E_{Ly}])$$

$$= \frac{\varepsilon_r \varepsilon_0}{2}\left([E_{1x} + E_{Lx}]^2 + \left[E_{1y} + E_{Ly}\right]^2\right) \quad (7)$$

3. Results

Here by using Eq 7 the density of the electric field energy, u_F, is calculated around two surface-charged spheres (where the smaller sphere is located inside the larger sphere) surrounded in- and outside by electrolyte. The radius of the larger and smaller sphere is: $R_L = 10^{-6}\, m$ and $R_1 = 0.2\, R_L$, respectively. The surface charge density of the homogeneously charged spheres is $\rho_s = -0.266\, C/m^2$ (the surface charge density of the PLFE lipid vesicles [1]). The total charge of the larger and the smaller sphere is, $Q_2 = \rho_s 4\pi R_2^2 = -3.3427 \cdot 10^{-12}\, C$ and $Q_1 = \rho_s 4\pi R_1^2 = -1.337 \cdot 10^{-13}\, C$, respectively. This system is axially symmetric, where the symmetry axis is the straight line connecting the centers of the spheres. The center of the attached coordinate system is at the center of large sphere and the x axis is defined by the symmetry axis. Because of the axial symmetry of the system it is enough to calculate u_F along straight lines parallel to the symmetry axis (see Figure 2), where the same y_P

coordinate belongs to each straight line. The surface-charged spheres are surrounded by electrolyte containing monovalent ions. The considered electrolyte ion concentrations (of the positive ion) are: 0.00001, 0.001 and $0.1\ mol/m^3$ and the respective Debye lengths are: $3.05 \cdot 10^{-6}$, $3.05 \cdot 10^{-7}$ and $3.05 \cdot 10^{-8}\ m$ (see Table 1 in ref.7), and the relative permittivity of the electrolyte is $\varepsilon_r = 78$.

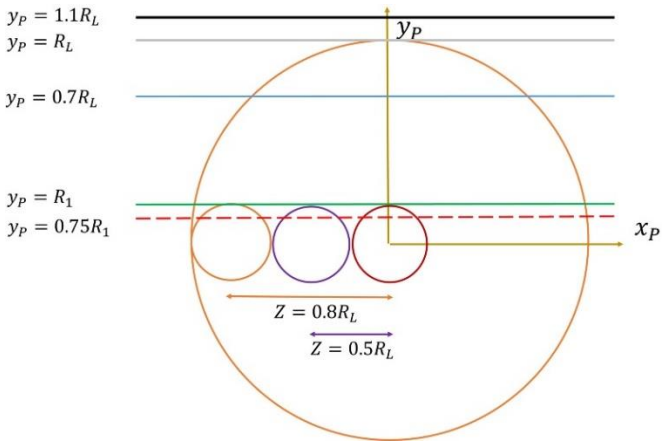

Figure 2. Locations of a small surface-charged sphere inside a large surface-charged sphere.

Inside a large surface-charged sphere of radius $R_L(= 10^{-6}\ m)$ a small surface-charged sphere of radius $R_1(= 0.2\ R_L)$ is located. The electric field energy density, u_F is calculated at the three different locations of the small sphere, i.e. in Figure 3, Figure 4 and Figure 5 the center of the small sphere is at $Z = 0.8\ R_L$ (see small orange circle), $Z = 0.5\ R_L$ (see small purple circle) and $Z = 0$ (see small dark red circle at the center of the large circle), respectively. In Figures 3–5 the electric field energy densities are calculated along the five horizontal (dashed red, green, blue, grey, black) lines.

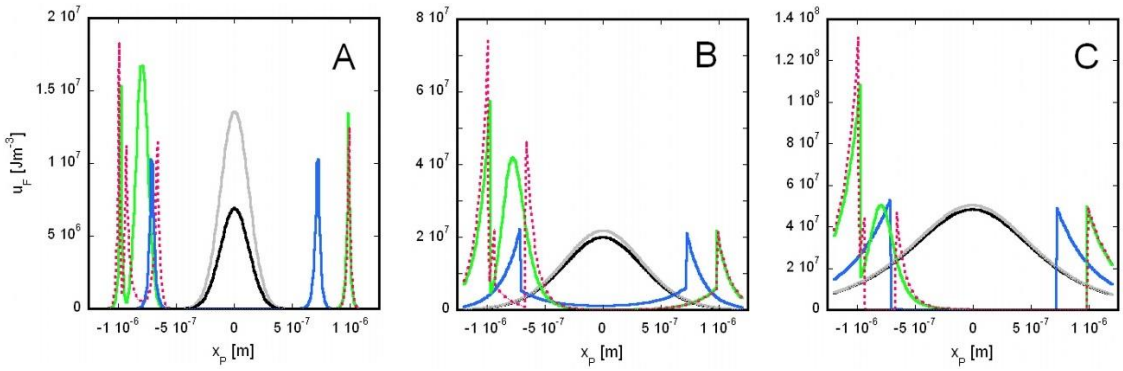

Figure 3. Density of the electric field energy around two surface-charged spheres.

$Z = 0.8\ R_L$

Dotted red line: $y_P = 0.75\ R_1$; green line: $y_P = R_1$; blue line: $y_P = 0.7\ R_L$; grey line: $y_P = R_L$; black line: $y_P = 1.01\ R_L$. The concentration of the monovalent positive (or negative) ion in the electrolyte is: A) $C = 0.1\ mol/m^3$; B) $C = 0.001\ mol/m^3$; C) $C = 0.00001\ mol/m^3$.

The connection point between the large sphere and the small sphere (represented by orange circle in Figure 2) is at $x_P = -R_L$ and $y_P = 0$. At this point there is no electrolyte and Eqs 4–7 are not

applicable. Similar situations take place when the horizontal line crosses the circles in Figure 2. The x_p coordinates of these cross sections, x_p^c can be calculated by:

$$x_p^c = \pm\sqrt{R_L^2 - y_p^2} \text{ (crossing the large circle, i.e. } y_P < R_L) \quad (8)$$

and

$$x_p^c = -Z \pm \sqrt{R_1^2 - y_p^2} \text{ (crossing the small circle located at } -R_L < x_1 < 0 \text{ and } y_P < R_1) \quad (9)$$

$$x_p^c = Z \pm \sqrt{R_1^2 - y_p^2} \text{ (crossing the small circle located at } 0 < x_1 < R_L \text{ and } y_P < R_1) \quad (10)$$

where x_1 is the x coordinate of the center of the small sphere.

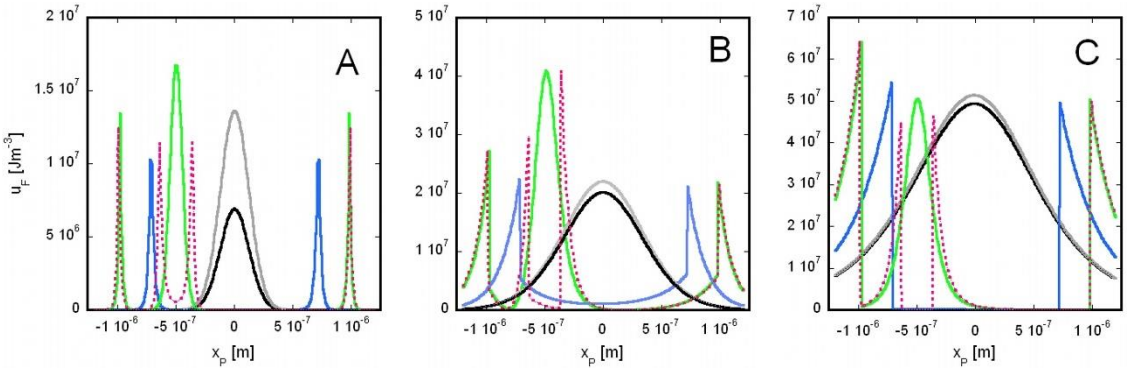

Figure 4. Density of the electric field energy around two surface-charged spheres.

$Z = 0.5\ R_L$

Dotted red line: $y_P = 0.75\ R_1$; green line: $y_P = R_1$; blue line: $y_P = 0.7\ R_L$; grey line: $y_P = R_L$; black line: $y_P = 1.01\ R_L$. The concentration of the monovalent positive (or negative) ion in the electrolyte is: A) $C = 0.1\ mol/m^3$; B) $C = 0.001\ mol/m^3$; C) $C = 0.00001\ mol/m^3$.

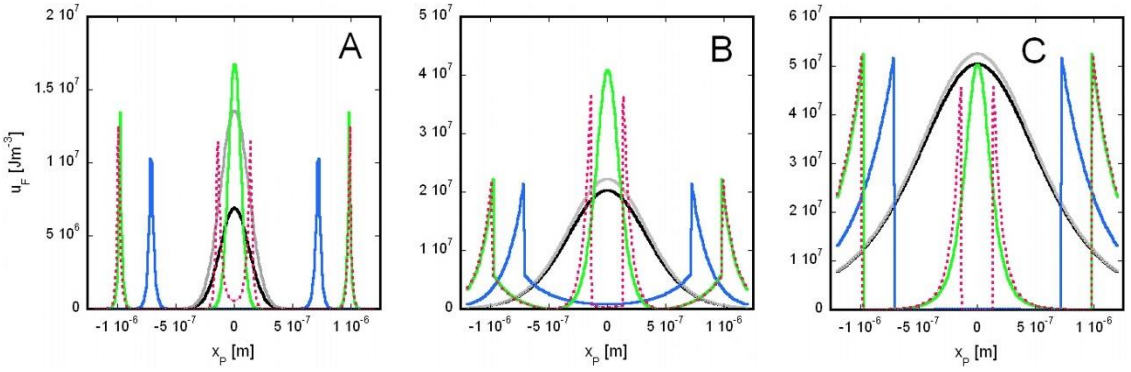

Figure 5. Density of the electric field energy around two surface-charged spheres.

$Z = 0$

Dotted red line: $y_P = 0.75\ R_1$; green line: $y_P = R_1$; blue line: $y_P = 0.7\ R_L$; grey line: $y_P = R_L$;

black line: $y_P = 1.01\,R_L$. The concentration of the monovalent positive (or negative) ion in the electrolyte is: A) $C = 0.1\,mol/m^3$; B) $C = 0.001\,mol/m^3$; C) $C = 0.00001\,mol/m^3$.

Note in Figures 3–5 the sharp maxima of the density of the electric field energy appear where the horizontal line at the respective y_P crosses the charged sphere(s). These crossing points, x_p^c's, can be calculated by Eqs 8–10. In the case of $y_P = 0.75\,R_1$ the values of the crossing points are listed at the first column of Table 1.

It is also important to note that $|\underline{E_1}| \sim Q_1$ and $|\underline{E_L}| \sim Q_L$ (see Eqs 4–6) and thus in the case of total surface charges $a \cdot Q_1$ and $a \cdot Q_L$ (where $0 < a < 1$ is a constant) the electric field energy density will be a^2 times of the above calculated $u_F(x_P, y_P)$ values (see Eq 7).

4. Discussion

In this work the solution of the screened Poisson equation ([7] and Eq A5 in Appendix 1) is used to calculate the field energy density around two surface-charged spheres where the small sphere is located inside the large sphere. This solution is not restricted to small potentials (<< 25 mV) like in the case of the Debye-Hückel approximation of the Poisson-Boltzmann equation [9] where the superposition principle is not applicable either. This is an important advantage because the measured absolute value of the Zeta potentials of the cells are usually higher than 25 mV (e.g. –57.89 ± 22.63 mV on ARO cells, –40.41 ± 5.10 mV on C32TG cells, −46.99 ± 18.71 mV on RT4 cells, –40.13 ± 9.28 mV on TK cells, and −43.03 ± 5.52 mV on UM-UC-14 cells [14].

The considered two spheres (with homogeneously charged surfaces) electrically interact. If the lateral movement of the charges on the spheres would not be restricted the interaction of the smaller sphere (located inside the larger sphere) with the larger sphere would result in inhomogeneous distribution of the surface charges on both spheres. However, the free lateral diffusion of proteins and lipids are usually restricted in biological membranes not only by direct collisions with structures where immobile proteins are crowded, but also by electrostatic deflection, hydrophobic mismatches, and other mechanisms [15].

The density of the electric field energy depends on the electric field strength (Eq 3), i.e. the gradient of the electric potential (Eqs 4,6). In the case of a single surface-charged sphere surrounded by electrolyte with low ion concentration the potential inside the sphere is close to constant (see red curve in Figure 3A in ref. [7]) and thus the absolute value of the electric field strength is close to zero. On the other hand, outside the sphere the absolute value of the potential and also the electric field strength decrease with increasing distance from the surface of the sphere (see red curve in Figure 3A in ref. [7]). At higher electrolyte ion concentration, because of the increased screening effect, the absolute value of the potential and also the electric field strength decrease faster with increasing distance from the surface of the sphere. In this case inside the sphere toward its center the absolute value of the potential and the electric field strength also decrease (see curves in Figure 3A,B in ref. [7]).

In this work two surface-charged spheres (with the same surface charge density) are considered where the smaller sphere is located inside the larger sphere. The above mentioned electric properties of a single surface-charged sphere remain the same for the smaller sphere (located inside a larger sphere) if the surfaces of the spheres are far enough from each other (farther than $4\,\lambda_D$), i.e. the absolute value of the potential decreases close to zero between the surfaces of the two spheres. However, when part of the surfaces of the two spheres are close enough to each other one sphere contributes to the potential and electric field strength around the other sphere. The electric field energy

density is particularly high at the place where the surfaces of the two spheres touch each other. This maximal electric field energy density is very close to the outer surface of the larger sphere. Thus one can detect at the outer surface of the erythrocyte when the nucleus is getting close.

The electric field energy density has maximum when the horizontal line crosses the circles in Figure 2. The x_p coordinates of these cross sections, x_p^c can be calculated by Eqs 8–10. When the x axis of the coordinate system is the horizontal line (i.e. $y_P = 0$) the electric field energy density is particularly high at the place where the surfaces of the two spheres touch each other (see orange circles in Figure 2) at close to zero electrolyte ion concentration (i.e. $C = 0.00001\ mol/m^3$):

$$u_F(x_P = -R_{L+}, y_P = 0; -x_1 = Z = 0.8R_L = R_L - R_1)$$

$$= \frac{\varepsilon_r \varepsilon_0}{2}(\cdot\,[E_{1x} + E_{Lx}]^2 + [E_{1y} + E_{Ly}]^2)$$

$$= \frac{\varepsilon_r \varepsilon_0}{2}\left(\left[\left(-\frac{dV_1}{dD_1}\right)_{D_1=R_{1+}} \frac{x_p - x_1}{R_{1+}} + \left(-\frac{dV_L}{dD_L}\right)_{D_L=R_{L+}} \frac{x_p}{R_{L+}}\right]^2 + [0+0]^2\right)$$

$$\cong \frac{\varepsilon_r \varepsilon_0}{2}\left(\left[-\frac{k_e Q_1}{\varepsilon_r R_{1+}^2} - \frac{k_e Q_L}{\varepsilon_r R_{L+}^2}\right]^2\right) = \frac{2\rho_S^2}{\varepsilon_r \varepsilon_0} = 1.4798 \cdot 10^8 Jm^{-3} \quad (11)$$

This maximal electric field energy density is very close to the outer surface of the larger sphere ($|x_P| = R_{L+} \geq R_L$) on the x axis of the coordinate system. The x axis also crosses the small and large spheres at $x_p = -3\ R_1$ and $x_p = R_L$, respectively. Very close to these coss sections, at the outer side of the spheres, the field energy density is only a quarter of the above maximal value.

In general the first maximum of u_F (see the left maximum in Figures 3–5) is getting smaller when the center of the small sphere approaches the center of the large sphere. This is the case because the interaction between the spheres is reducing when the average distance between the surfaces of the two spheres is increasing.

In the case of horizontal lines where $y_P > 0$ $E_{1y} + E_{Ly}$ contributes also to u_F. This contribution is particularly high by E_{1y} when $x_p \cong -Z$ or by E_{Ly} when $x_p \cong 0$ relative to the contribution by E_{1x} and E_{Lx}, respectively.

When the location of the center of the small and large sphere is identical (i.e. $Z = 0$) then because of the additional symmetry $u_F(x_P, y_P) = u_F(-x_p, y_P)$ at any value of y_p (see Figure 5).

When $y_p > R_1$the horizontal line crosses only the surface of the large sphere at two points and these are symmetric crossing points (where the y axis is the symmetry axis). The distance of the left crossing point from the y axis is similar to the distance of the right crossing point from the y axis (see Eq 8). Because of this symmetry if the small sphere only slightly affect the field strength along the horizontal line then $u_F(x_P, y_P) \cong u_F(-x_p, y_P)$ at any location of the small sphere along the x axis (see blue, black and grey lines in Figures 3–5).

In the case of $0 < y_p < R_1$ the horizontal line crosses twice the large and twice the small sphere. In the case of the dotted red lines in Figures 3–5 $y_p = 0.75\ R_1$ and each curve has four maxima. The hight of each maxima depends on the square of the field strength at the respective crossing point (see Eq 3), which is related to the x and y components of the field strengths created by the small sphere (E_{1x}, E_{1y}) and by the large sphere (E_{Lx}, E_{Ly}) (see Eq 7). In order to find out the reason of the hight of each maximum of the curves shown in Figures 3B–5B (i.e. at $C = 0.001\ mol/m^3$) in Table 1 these x and y components of the field strengths are listed.

Table 1. Values of the x and y components of the electric field strength at the cross sections between a horizontal line (at $y_p = 0.75 \cdot R_1$) and two spheres of radii R_1 and R_L.

Cross #	$x_P\ [m]$	$u_F\ [J]$	$E_{1x}\ [V/m]$	$E_{Lx}\ [V/m]$	$E_{1y}\ [V/m]$	$E_{Ly}\ [V/m]$
			$Z = 0.8\ R_L$			
1	$-9.9 \cdot 10^{-7}$	$7.4 \cdot 10^{7}$	$1.8 \cdot 10^{8}$	$2.47 \cdot 10^{8}$	$-1.42 \cdot 10^{8}$	$-3.74 \cdot 10^{7}$
2	$-9.4 \cdot 10^{-7}$	$2.2 \cdot 10^{7}$	$2.29 \cdot 10^{8}$	$-1.16 \cdot 10^{8}$	$-2.45 \cdot 10^{8}$	$1.86 \cdot 10^{7}$
3	$-6.6 \cdot 10^{-7}$	$4.65 \cdot 10^{7}$	$-2.29 \cdot 10^{8}$	$-5.45 \cdot 10^{7}$	$-2.45 \cdot 10^{8}$	$1.24 \cdot 10^{7}$
4	$9.9 \cdot 10^{-7}$	$2.15 \cdot 10^{7}$	$-9.7 \cdot 10^{4}$	$-2.47 \cdot 10^{8}$	$-8.2 \cdot 10^{3}$	$-3.74 \cdot 10^{7}$
			$Z = 0.5\ R_L$			
1	$-9.9 \cdot 10^{-7}$	$2.73 \cdot 10^{7}$	$3 \cdot 10^{7}$	$2.47 \cdot 10^{8}$	$-9.22 \cdot 10^{6}$	$-3.74 \cdot 10^{7}$
2	$-6.4 \cdot 10^{-7}$	$2.97 \cdot 10^{7}$	$2.29 \cdot 10^{8}$	$-5.16 \cdot 10^{7}$	$-2.45 \cdot 10^{8}$	$1.2 \cdot 10^{7}$
3	$-3.6 \cdot 10^{-7}$	$4.1 \cdot 10^{7}$	$-2.29 \cdot 10^{8}$	$-2.2 \cdot 10^{7}$	$-2.45 \cdot 10^{8}$	$9.16 \cdot 10^{6}$
4	$9.9 \cdot 10^{-7}$	$2.15 \cdot 10^{7}$	$-3.2 \cdot 10^{5}$	$-2.47 \cdot 10^{8}$	$-3.22 \cdot 10^{4}$	$-3.74 \cdot 10^{7}$
			$Z = 0.0\ R_L$			
1	$-9.9 \cdot 10^{-7}$	$2.2 \cdot 10^{7}$	$2.6 \cdot 10^{6}$	$2.47 \cdot 10^{8}$	$-3.97 \cdot 10^{5}$	$-3.74 \cdot 10^{7}$
2	$-1.4 \cdot 10^{-7}$	$3.63 \cdot 10^{7}$	$2.29 \cdot 10^{8}$	$-7.6 \cdot 10^{6}$	$-2.45 \cdot 10^{8}$	$8.17 \cdot 10^{6}$
3	$1.4 \cdot 10^{-7}$	$3.63 \cdot 10^{7}$	$-2.29 \cdot 10^{8}$	$7.6 \cdot 10^{6}$	$-2.45 \cdot 10^{8}$	$8.17 \cdot 10^{6}$
4	$9.9 \cdot 10^{-7}$	$2.2 \cdot 10^{7}$	$-2.6 \cdot 10^{6}$	$-2.47 \cdot 10^{8}$	$-3.97 \cdot 10^{5}$	$-3.74 \cdot 10^{7}$

For example in the case of $Z = 0.5\ R_L$ (thus $x_1 = -Z = -5 \cdot 10^{-7}\ m$) the reason that the maximum at cross section 3 is higher than at cross section 2 is that at cross section 3 both $E_{1x}(3)$ and $E_{Lx}(3)$ are negative while at cross section 2 $E_{1x}(2)$ is positive and $E_{Lx}(2)$ is negative. Because of this at cross section 3 $[E_{1x} + E_{Lx}]^2$ much larger than at cross section 2. Actually because of the symmetry $|E_{1x}(3)| = |E_{1x}(2)|$ but $signE_{1x}(3) \neq signE_{1x}(2)$ because $sign\left(\frac{x_p(3)-x_1}{D_1}\right) \neq sign\left(\frac{x_p(2)-x_1}{D_1}\right)$ (see Eq 4).

As an other example in the case of $Z = 0.0\ R_L$ the maximum at cross section 3 is higher than at cross section 4. The reason is that $\left|E_{Ly}(4)\right| \ll |E_{Lx}(4)|$ while $\left|E_{1y}(3)\right| \cong |E_{1x}(3)| \cong |E_{Lx}(4)|$. Note that $\left|E_{Ly}(4)\right| \ll |E_{Lx}(4)|$because the direction of $\underline{E_L}(4)$ is close to the direction of the x axis.

Finally, the analytical equation, Eq 7, for the calculation of the electric field energy density of two surface-charged spheres (the smaller sphere located inside the larger sphere), can be generalized for the case when N small surface-charged spheres are located inside the large sphere (see Appendix 2). Also when the radius of the smaller sphere approaches zero the total surface charge of the smaller sphere, Q_1 approaches zero too and consequently the electric field strength of the smaller sphere, $\underline{E_1}$approaches zero. Thus, based on Eq 7 one can calculate the field energy density around a single charged sphere by:

$$u_F(x_P, y_P) = \frac{\varepsilon_r \varepsilon_0}{2} \underline{E} \cdot \underline{E} = \frac{\varepsilon_r \varepsilon_0}{2} \left(\underline{E_L}\right) \cdot \left(\underline{E_L}\right)$$

$$= \frac{\varepsilon_r \varepsilon_0}{2} (E_{Lx}, E_{Ly}) \cdot (E_{Lx}, E_{Ly})$$

$$= \frac{\varepsilon_r \varepsilon_0}{2} \left([E_{Lx}]^2 + \left[E_{Ly}\right]^2 \right)$$

5. Conclusions

Based on the generalized version of Newton's Shell Theorem [7] the electric field energy density, u_F around two surface-charged spheres surrounded by electrolyte where the smaller sphere is inside the larger one is analytically calculated. According to the calculations when the surfaces of the spheres are farther from each other than four times of the Debye length the field energy density around and inside the smaller sphere is basically independent from the presence of the larger sphere. The electric field energy density is maximal when the smaller sphere touches the inner surface of the larger sphere and the maximum of u_F is located at the touching point on the outer surface of the larger sphere.

Acknowledgments

The author is very thankful for Chinmoy Kumar Ghose.

Conflict of interest

The author declares no conflict of interest.

References

1. Chong PLG (2010) Archaebacterial bipolar tetraether lipids: Physico-chemical and membrane properties. *Chem Phys Lipids* 163: 253–265. https://doi.org/10.1016/j.chemphyslip.2009.12.006
2. Ewald PP (1921) Die berechnung optischer und elektrostatischer gitterpotentiale. *Ann Phys-berlin* 369: 253–287. https://doi.org/10.1002/andp.19213690304
3. Sugár IP, Thompson TE, Biltonen RL (1999) Monte carlo simulation of two-component bilayers: DMPC/DSPC mixtures. *Biophys J* 76: 2099–2110. https://doi.org/10.1016/S0006-3495(99)77366-2
4. Almeida PFF (2009) Thermodynamics of lipid interactions in complex bilayers. *BBA-Biomembranes* 1788: 72–85. https://doi.org/10.1016/j.bbamem.2008.08.007
5. Bohinc K, Špadina M, Reščič J, et al. (2022) Influence of charge lipid head group structures on electric double layer properties. *J Chem Theory Comput* 18: 448–460. https://doi.org/10.1021/acs.jctc.1c00800
6. Newton I (1999) *The Principia: Mathematical Principles of Natural Philosophy*, Berkeley: University of California Press, 590.
7. Sugár IP (2020) A generalization of the shell theorem. Electric potential of charged spheres and charged vesicles surrounded by electrolyte. *AIMS Biophys* 7: 76–89. https://doi.org/10.3934/biophy.2020007
8. Fetter AL, Walecka JD (2003) *Theoretical Mechanics of Particles and Continua*, New York: Dover Publications, 307–310.
9. Holtzer AM (1954) The collected papers of Peter JW Debye. Interscience, New York-London, 1954. xxi+ 700 pp., $9.50. *J Polym Sci* 13: 548. https://doi.org/10.1002/pol.1954.120137203
10. Sugár IP (2021) Electric energies of a charged sphere surrounded by electrolyte. *AIMS Biophys* 8: 157–164. https://doi.org/10.3934/biophy.2021012

11. Ma Y, Poole K, Goyette J, et al. (2017) Introducing membrane charge and membrane potential to T cell signaling. *Front Immunol* 8: 1513. https://doi.org/10.3389/fimmu.2017.01513
12. Bar-Shavit Z (2007) The osteoclast: a multinucleated, hematopoietic-origin, bone-resorbing osteoimmune cell. *J Cell Biochem* 102: 1130–1139. https://doi.org/10.1002/jcb.21553
13. Griffiths DJ (2005) Introduction to electrodynamics. *AM J Phys* 73: 574. https://doi.org/10.1119/1.4766311
14. Nishino M, Matsuzaki I, Musangile FY, et al. (2020) Measurement and visualization of cell membrane surface charge in fixed cultured cells related with cell morphology. *PLoS One* 15: e0236373. https://doi.org/10.1371/journal.pone.0236373
15. Trimble WS, Grinstein S (2015) Barriers to free diffusion of proteins and lipids in plasma membrane. *J Cell Biol* 208: 259–271. https://doi.org/10.1083/jcb.201410071

AIMS Press